*Published online 15 October 2010* *Nucleic Acids Research, 2011, Vol. 39, No. 6* ***1993–2006***
*doi:10.1093/nar/gkq864*

# Chromatin and DNA methylation dynamics during retinoic acid-induced RET gene transcriptional activation in neuroblastoma cells

**T. Angrisano[1], S. Sacchetti[2], F. Natale[1], A. Cerrato[1], R. Pero[1], S. Keller[1,2], S. Peluso[1], B. Perillo[3], V. E. Avvedimento[1], A. Fusco[1,2], C. B. Bruni[1], F. Lembo[4], M. Santoro[1] and L. Chiariotti[1,2,4,*]**

[1]Dipartimento di Biologia e Patologia Cellulare e Molecolare and Istituto di Endocrinologia ed Oncologia Sperimentale CNR, Università degli Studi di Napoli 'Federico II' 80131 Naples, [2]Naples Oncogenomic Center, CEINGE Biotecnologie Avanzate, Naples, [3]Istituto di Scienze dell'Alimentazione, Consiglio Nazionale delle Ricerche, 83100 Avellino and [4]Dipartimento di Chimica Farmaceutica e Tossicologica, Facoltà di Farmacia, Università degli Studi di Napoli 'Federico II' 80131 Naples, Italy

Received March 19, 2009; Accepted September 14, 2010

## ABSTRACT

**Although it is well known that RET gene is strongly activated by retinoic acid (RA) in neuroblastoma cells, the mechanisms underlying such activation are still poorly understood. Here we show that a complex series of molecular events, that include modifications of both chromatin and DNA methylation state, accompany RA-mediated RET activation. Our results indicate that the primary epigenetic determinants of RA-induced RET activation differ between enhancer and promoter regions. At promoter region, the main mark of RET activation was the increase of H3K4me3 levels while no significant changes of the methylation state of H3K27 and H3K9 were observed. At RET enhancer region a bipartite chromatin domain was detected in unstimulated cells and a prompt demethylation of H3K27me3 marked RET gene activation upon RA exposure. Moreover, ChIP experiments demonstrated that EZH2 and MeCP2 repressor complexes were associated to the heavily methylated enhancer region in the absence of RA while both complexes were displaced during RA stimulation. Finally, our data show that a demethylation of a specific CpG site at the enhancer region could favor the displacement of MeCP2 from the heavily methylated RET enhancer region providing a novel potential mechanism for transcriptional regulation of methylated RA-regulated loci.**

## INTRODUCTION

Retinoids play a critical role in cell proliferation, differentiation and apoptosis in normal tissues during embryonic development (1–3). Retinoic acid (RA) induces differentiation in many cell types and is the most widely used differentiating therapeutic agent (4). RA effects are mediated by two families of nuclear RA receptors, RARs and RXRs, which function as homo/heterodimers and directly modulate transcriptional activity by binding to RA responsive elements (RAREs) (5). Different studies indicate that epigenetic modifications play important roles in RA transcriptional regulation (6–10). In the absence of RA, corepressive elements (SMRT, NCoR and Sin3A) inhibit transcription while the presence of RA releases corepressors and histone deacetylases allowing chromatin remodelling and access to specific RAREs (8,9). Recently, it has been reported that topoisomerase II and poly (ADP-ribose) polymerase 1 collaborate to create a double-strand break at a RA target promoter (RARB) necessary for RAR-mediated transcription (11). The epigenetic dynamics of RA-induced Hox genes, that contain canonical RARE in the enhancer regions, has been also studied (12,13). It has been demonstrated that polycomb group repressive complexes (PRC1 and PRC2/3) participate to transcriptional regulation of Hox genes. In particular, it is thought that trimethylation of lysine 27 (K27)

*To whom correspondence should be addressed. Tel: +39 81 7462056; Fax: +39 81 7703285; Email: chariot@unina.it

The authors wish it to be known that, in their opinion, the first three authors should be regarded as joint First Authors.

of histone H3 (H3K27me3), caused by EZH2, a component of PRC2/3 complex, serves as a binding site for recruitment of PRC1 complex leading to repression of Hox genes. Recently, it has been demonstrated that RA treatment of F9 embryonal carcinoma cells causes recruitment of pCIP, p300 and RNA polymerase II at target RAREs occurring together with the displacement of SUZ12, a component of PRC2/3 repression complex (13). However, to date a limited number of information are available on the epigenetic dynamics of RA response compared to the extensive studies addressing the dynamics of transcriptional activation mediated by other nuclear receptors (most notably estrogen receptor) in response to ligand (14,15)

In this work, we have investigated the major epigenetic modifications occurring at RET locus in a neuroblastoma cell line upon RA stimulation. Neuroblastic tumors show dramatic neural maturation in response to RA through the transcriptonal regulation of genes involved in the differentiation process (16–19). In particular, RET, a tyrosine kinase receptor, is consistently up-regulated upon RA treatment of different neuroblastoma cell lines (19). Because interference with RET activation affects the whole RA-induced transcriptional and differentiation programs (19), RET is considered to play a key role in this process. The general structure of human RET gene and the main regulatory elements have been partially investigated and it has been reported that a conserved enhancer region, located about 3000-bp upstream from a promoter region, contains binding sites for Sox10 and Pax3 transcription factors (20–22). However, the mechanisms leading to RET activation by RA in neuroblastoma cells are still poorly understood. Here we show that a complex series of epigenetics events, that include both chromatin and DNA methylation modifications, accompany RA-mediated RET activation.

## MATERIALS AND METHODS

### Cell culture

SK-N-BE cells were cultured in Dulbecco's Modified Eagle's Medium supplemented with 10% foetal bovine serum (Life Technologies), 2 mM glutamine, penicillin (25 U/ml) and streptomycin (25 μg/ml) in a 5% $CO_2$ atmosphere at 37°C. All the treatments with all-trans RA (Sigma-Aldrich) were performed using a 10 μM final concentration. 5-Aza-2-deoxyazacytidine (ICN Biomedical Inc.) treatments were performed for 48 h at 10 μM or 50 μM final concentration.

### Construction of fusion genes

pEISP-RET construct was obtained by amplifying the Enhancer-IS-Promoter sequence of RET (nt −3221 to +167) by PCR and then subcloned in the KpnI restriction site of pGL3-basic Luciferase Vector (Promega). Primers used were: EISP-KpnI/Fw: 5′-ATTGGTACCAACCATGCTTCTCAGTGCAGGC-3′; EISP-KpnI/Rv: 5′-ATTGGTACCACGGCTGGAGGGACTGCGGCTAG-3′ (underlined the restriction sites for cloning). Plasmids pRARE-wt and pRARE-Mut were obtained cloning the potential binding region of RARα (RARE), found by bioinformatic search, into pGL3-promoter Luciferase Vector. Primers used for the amplification of RARE region (RARE-wt, from −3178 to −3046) containing each a DR of the identified putative RARE (bold) and a tag with restriction sites for cloning (underlined), were: RARE-wt-MluI/FW: 5′-TTTAGACGCGTCCCCCATGTCACCT**GGGTCA**GAGGAC-3; RARE-wt-XhoI/RV: 5′-AAATGGCTCGAGGGAGCACCTCAGGTC**TGAC****C**CCAAAGC-3′. pGL3-RAREwt was then generated by inserting the MluI/XhoI digested amplicon in the same sites of pGL3-promoter Luciferase Vector.

To obtain a mutant version of RARE region we used other two oligos, similar to those indicated above, but both carrying a mutation by deletion of three nucleotides belonging to the DR (residued DR's nucleotides are indicated in bold): RARE-MUT-MluI/FW: 5′-TTTAGACGCGTCCCCCATGTCACCT**GGG**GAGGACACAGAGCATC-3′; RARE-MUT-XhoI/RV: 5′-AAATGGCTCGAGGGAGCACCTCAGGTC**CCC**CAAAGCACCAAAACG-3′. pGL3-RARE-Mut was then constructed by inserting the MluI/XhoI digested amplicon in the same sites of pGL3-promoter Luciferase Vector. All constructs were verified by DNA sequencing.

### Transient transfections and luciferase assays

SK-N-BE cells were transiently transfected using Lipofectamine™ 2000 CD Reagent (Invitrogen) in a 24-well plates. At 70% of confluence, in 500 μl of growth medium, the cells were transfected with the reporter construct pGL3-promoter Luciferase Vector (Promega). Co-transfections were carried out in the presence of 200 ng of reporter construct and 200 ng of Renilla construct and with or without 200 ng of pRARE-wt, pRARE-Mut or pEISP-RET. Luciferase and Renilla activities were measured with the dual-luciferase reporter assay kit (Promega, Madison, WI, USA), and expressed as relative to untreated control cells as Relative Luciferase Units.

### Statistical analysis

Statistical significance between groups was assessed by Student's test. Data are expressed as means ± SD. All experiments were repeated at least three times. A $P$-value $<0.05$ or $<0.01$ was considered to be statistically significant.

### Antibodies

Antibodies used for all ChIP assays were: anti-H3Ac (#06-599), anti di-methyl-H3K9 were from Upstate (Upstate Biotechnology, Dundee; UK). Anti-RARα (N-20, sc-551), anti-HDAC1 (C-19, sc-6298) and anti-mSin3A (AK-11, sc-767) antibodies were from Santa Cruz Biotechnology (Santa Cruz, CA, USA). Anti-di-methyl-H3K4 (ab7766), anti-tri-methyl-H3K4 (ab8580), anti-tri-methyl-H3K9 (ab8898), anti-MeCP2 (ab2828), MBD2 (ab3754), anti-Dnmt1 (ab16632) and anti-Dnmt3b (ab2851) were from Abcam Inc. (Cambridge, MA, USA). Anti-tri-methyl-H3K27 (AM-0174-200) antibody was from Lake Placid

Biologicals (Lake Placid, NY, USA) and anti-EZH2 (3147) antibody was from Cell Signaling (Danvers, MA, USA). The specificity of anti-HDAC1, MeCP2, EZH2, Sin3a, DNMT1 and DNMT3b antibodies was assessed by western-blot analysis of SK-N-BE cell lysates (data not shown).

### Real Time RT–PCR

Total RNA was isolated with RNeasy extraction kit Qiagen (Qiagen, GmBh) according to the manufacturer instructions. The integrity of the RNA was assessed by denaturing agarose gel electrophoresis and spectrophotometry. To ensure that RNA samples were not contaminated by DNA, negative controls were obtained by performing the PCR on samples that were not reversed-transcribed but otherwise identically processed. One microgram of total RNA of each sample was reverse-transcribed with QuantiTect® Reverse Transcription (Qiagen) using an optimized blend of oligo-dT and random primers according to the manufacturer's instructions. Quantitative PCR amplifications were performed using QuantiTect SYBR Green (Qiagen) in a Chromo4 Real Time thermocycler (BIORAD). Following primers were used for RET amplifications: RET1f (forward) 5′-TGCATCCAGGAGGACACC-3′ and RET1r (reverse) 5′-TTGAGGTAGACGGTGAGC AG-3′. MeCP2: Hs_MECP2_1_SG QuantiTec primer assay QT00039361 (Qiagen). G6PD gene was used as housekeeping gene; following primers were used for PCR reaction: G6PDf (forward) 5′-GCAAACAGAGTG AGCCCTTC-3′ and G6PDr (reverse) 5′-ggccagc cacataggagtt-3′. The conditions used for PCR were 2 min at 95°C, and then 45 cycles of 20 s at 95°C and 1 min at 60°C. Each reaction was performed in triplicates. Calculations of relative expression levels were performed using the $2^{-\Delta\Delta Ct}$ method (23) taking into account the values of at least three independent experiments.

### Gene silencing by RNA interference

SK-N-BE cells were plated at a density of $6 \times 10^5$ per 60-mm culture dish 24 h before transfections. Cells were transfected with MeCP2 siRNA (Qiagen, Hs_MeCP2_7, SI02664893, target sequence: ACGGAGCGGATTGCAA AGCAA) or AllStars negative Control siRNA (Qiagen, 1027281) at a final concentration of 5 nM using HiPerfect Transfection reagent (Qiagen) according to the manufacturer's instructions. Cells were harvested after 48 h. RNA isolation and real-time PCR analyses were performed as described earlier.

### Quantitative ChIP analyses

Cells were cross-linked by adding 1% formaldehyde for 15 min at room temperature in shaking. Glycine was added to a final concentration of 125 mM for 5 min at room temperature in shaking. Cells were rinsed twice with cold PBS supplemented with 500 µM PMSF and harvested in five pellet volumes of Cell Lysis Buffer (5 mM PIPES pH 8.0, 85 mM KCl, 0.5% NP40) supplemented with 1 mM PMSF and Complete™ protease inhibitors mix (Roche). For each time point, four dishes containing $\sim 3–5 \times 10^6$ cells each, were utilized. Lysates were incubated for 30 min at 4°C and then passed through 10 dounce cycles. They were subsequently centrifuged and nuclei were collected. Nuclei were then resuspended in Sonication Buffer (0.3% SDS, 10 mM EDTA and 50 mM Tris–HCl pH 8.0) supplemented with 1 mM PMSF and Complete™ protease inhibitors mix (Roche, Indianapolis, IN, USA) and incubated for 60 min at 4°C. Chromatin was sonicated to an average DNA length of 400–600 bp using a 3 mm (small size) tip equipped Bandelin Sonoplus UW-2070 sonicator with $7 \times 15$ s cycles of pulses (specific cycle 0.3, Power 30%) alternated by 60 sec of rest. Sonicated samples were centrifuged and the supernatant was collected. Eighty micrograms of chromatin were diluted with Dilution Buffer (0.01% SDS, 1.2 mM EDTA and 16.7 mM Tris–HCl pH 8.0), precleared (2 h) by incubation with 20 µl Salmon Sperm DNA/Protein A Agarose-50% Slurry (#16-157, Upstate) and subjected to immunoprecipitation with specific antibodies with rotation overnight at 4°C. Immunocomplexes were collected by adsorption onto 30 µl Salmon Sperm DNA/Protein A Agarose-50% Slurry (#16-157, Upstate) and the beads were washed sequentially with Low Salt Washing Buffer (0.1% SDS, 2mM EDTA, 20 mM Tris–HCl pH 8.0, 1% Triton X-100 and 150 mM NaCl) (4 times), High Salt Washing Buffer (0.1% SDS, 2mM EDTA, 20 mM Tris–HCl pH 8.0, 1% Triton X-100 and 500 mM NaCl) (4 times) and LiCl Washing Buffer (#20-156, Upstate). Precipitates were washed with TE Buffer (10 mM Tris–HCl pH 8.0 and 1 mM EDTA), and antibody-chromatin fragments were eluted from the beads with 1% sodium dodecyl sulphate in 0.1 M $NaCO_3$. Cross-links were reverted by adding 200 mM NaCl and heating at 65°C overnight. 40 mg/ml RNase A and 20 mg/ml proteinase K, 10 mM EDTA and 40 mM Tris–HCl pH 6.5 were added and samples were then incubated for 2 h at 45°C. Samples were then extracted in phenol-chloroform-isoamylic alcohol (25:24:1), ethanol-precipitated and finally centrifuged at 13 000 rpm for 45 min at 4°C. Pellets were washed with 70% ethanol, centrifuged at 8000 rpm for 5 min at 4°C and finally resuspended in 60 µl of $H_2O$. For subsequent PCR analysis, 2 µl of each sample were used as template. Following primers were used for amplification: EQuF 5′-C ACCGACCACTTTGCTAACAG-3′ (position from nts −3475 to −3454) and EQuR 5′-GGTGGTTGGAAGCA CAGACT-3′(position from −3435 to −3416) for the analysis of enhancer region; IQuF 5′-AGGAGCACAGC CCCAGAT-3′ (position from nts −1691 to −1674) and IQuR 5′-GCCCTTGGCTGACATTGA-3′ (position from nts −1636 to −1619) for IS; PQuF 5′-ATTCGTGCGGA GAGTTCTGTT-3′ (position from nts +652 to +667) and PQuR 5′-CTGAGCGGGAAAAGGAAAC-3′ (position from nts +697 to +715) for promoter region; immunoprecipitations with IgG were used as negative controls. The signals obtained by precipitation with the control IgG was subtracted from the signals obtained with the specific antibodies. Results are expressed as percentage of the input, and calculations take into account the values of at least three independent experiments.

### DNA methylation analysis

Genomic DNA was isolated with DNeasy extraction kit (Qiagen) according to the manufacturer instructions. Sodium bisulfite conversion was performed by using EZ DNA Methylation Kit (Zymo Research). The manufacture's protocol was followed by using 2 μg of genomic DNA and eluted in 30 μl of $H_2O$.

*Bisulphite genomic sequencing*. Two microliters of each sample was used as template in PCR reactions using the following primers: EbiF 5′-tagtggtagatagatgggaaattgag g-3′ (position from nts −3502 to −3476) and EbiR 5′-cct aaaacacctcaaatctaaccccaaaacac-3′(from nts −3054 to −3023) for the analysis of RET enhancer region. PbiF 5′-gagagtttttttgtgtaagggatgtaaggg-3′ (position from nts −779 to −750) and PbiR 5′-cccrcttacaatccctacctttttac cctttcc-3′ (from nts −389 to −358) were used for the analysis of RET promoter region. Amplifications were carried out on 10 ng of bisulphite treated DNA using HotStarTaq DNA polymerase (Qiagen) under the following conditions: 15 min at 95°C, followed by 50 cycles of 30 s at 95°C, 52 s at 59°C and 1 min at 72°C, then a final elongation of 10 min at 72°C before holding at 4°C, in a final reaction volume of 30 μl. Confirmation of PCR product quality and freedom from contamination was established on 2% agarose gels with ethidium bromide staining. PCR final products were then cloned into the pGEM-T-easy vector provided by Promega pGEM®-T-Easy Vector System II (Promega Italia, Milan, Italy) following the supplier's procedures. Plasmid DNA was purified using the Qiagen plasmid Mini Kit. The purified plasmids were sequenced in both directions using T7 and Sp6 primers. At least 20 independent clones were sequenced to determine the methylation pattern of individual molecules. Sequencing was performed at the CEINGE Sequencing Core Facility.

Bisulfite analyses of MeCP2 immunoprecipitated DNA (ChIP-BA) were performed as previously described (24) using anti MeCP2 antibodies (ab2828-100, Abcam Inc, Cambridge MA, USA). In this case primers EbiF and EbiR2 (5′-cacattcaaaaacrcaactcratcctaataatac-3′) (position from −3320 to −3287) were used for amplification of bisulfite treated coimmunoprecipitated DNA.

*Pyrosequencing™ analysis*. Quantitative DNA methylation analysis was performed using the PSQ 96MA instrument from Pyrosequencing (Biotage AB, Uppsala, Sweden) following the protocol suggested by the manufacturer. The reactions were assayed on the PSQ™ 96MA using the SNP analysis software provided by the manufacturer. Primers used for PCR reactions were: EPyF 5′-agggtagtggtagata-3′ (position from nts −3506 to −3487) (5′-Biotinylated) and EPyR 5′- acycaactcyatccta ataatac-3′ (from nts −3298 to −3321). Amplifications were carried out on 10 ng of bisulphite treated DNA using HotStarTaq DNA polymerase (Qiagen) under the following conditions: 15 min at 95°C, followed by 50 cycles of 30 sec at 95°C, 52 sec at 59°C and 1 min at 72°C, then a final elongation of 10 min at 72°C before holding at 4°C, in a final reaction volume of 30 μl. Confirmation of PCR product quality and freedom from contamination was established on 2% agarose gels with ethidium bromide staining. PCR final products (208 bp) were then used for Pyrosequencing reactions; sequencing primers were: EPySeq1 5′-cattcctaaaactactaac -3′ (position from nts −3354 to −3336) and EPySeq2 5′-aactaactatatacactatt-3′ (position from −3459 to −3440). Target CpGs were evaluated by analysis of the resulting pyrograms. The analysis of a non-CpG cytosine provided an internal control of the completeness of bisulfite treatment.

*SEQUENOM MassARRAY platform*. This system utilizes MALDI-TOF mass spectrometry in combination with RNA base specific cleavage (MassCLEAVE). A detectable pattern is then analyzed for methylation status. PCR primers to analyze RET enhancer region (lower strand), designed by using Methprimer (http://www.urogene.org/methprimer) were: EmaF 5′-aggaagagagTG TTTTTTGATTTAGGTGATATGGG-3′ and EmaR 5′-cagtaatacgactcactatagggagaaggctAACCCCTCTAAAT ACCCTAAAAACC-3′. For reverse primer, an additional T7 promoter tag for *in vivo* transcription was added, as well as a 10-mer tag on the forward primer to adjust for melting-temperature differences. The MassCLEAVE biochemistry was performed as previously described (25). Mass spectra were acquired by using a MassARRAY Compact MALDI-TOF (Sequenom) and spectra's methylation ratios were generated by the Epityper software v1.0 (Sequenom). The whole procedure was performed at Sequenom GmbH Laboratories (Hamburg, Germany).

### Databases

RET gene sequences were retrieved by the Ensembl database (accession number: ENSG00000165731).

## RESULTS

### RARα associates with the RET gene upstream regulatory regions

It is known that RET gene is strongly activated by RA in neuroblastoma cells (19). In order to investigate whether RA receptors (RARs) can directly bind to RET regulatory regions, we first performed a bioinformatic analysis to identify potential RA responsive elements (RAREs) within the RET gene sequences (Figure 1A). Such analysis showed that a potential RARE is located, on the forward strand, at position −3178 to −3046 with the respect of transcriptional start site (TSS). This RARE is composed by two canonical hemi-sites but the distance between the two half-sites was 121 nt and not 5 nt as more frequently found in functionally characterized RAREs (26). Consensus sequences represented by two half-sites separated by up to 150 nt (DR150) have been identified as functional RAREs (27). We then performed chromatin immunoprecipitation (ChIP) experiments to verify the presence of RARα, in RA-stimulated and unstimulated cells, at three different regions of RET locus (Figure 1A): (i) the enhancer region located about 3.4-kb upstream from the TSS, containing functional SOX10 and

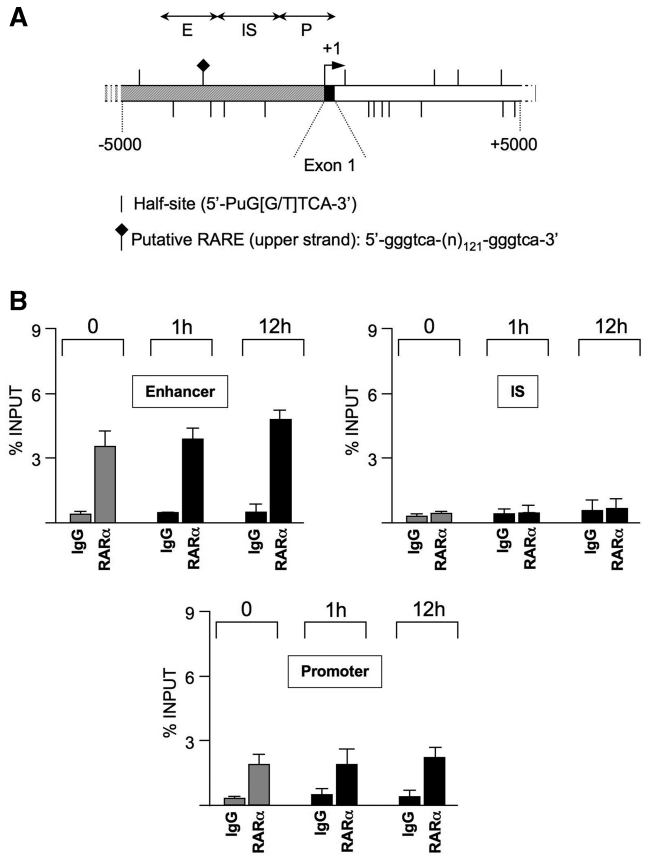


**Figure 1.** RARα association to RET gene regulatory regions. (**A**) Bioinformatical analysis. In the aim to find putative RARE we performed the analysis on both forward and reverse strand of the genomic region located between −5000 to +5000 nt positions with respect of RET trascriptional start site. We searched for all 5′-PuG[G/T]TCA-3′ motifs (half-sites) and considered only exact directly repeated half-sites separated by up to 150 nt as potential RARE sites. With these criteria only one putative RARE was identified on the forward strand, at position from −3178 to −3046, as indicated in the figure. E, Enhancer region; I, intervening sequences; P, Promoter region. (**B**) SK-N-BE cells were treated for 1 or 12 h with 10 μM RA or were left untreated (Time 0). ChIP experiments were performed with anti-RARα antibodies or with IgG (as negative control) and with region-specific primers (EQF and EQR for enhancer; IQF and IQR for IS; PQF and PQR for promoter). Primers to RAREs of human RARB and primers to exon 2 of the same gene were used as positive and negative controls, respectively. RARα levels at RARB RARE was about 30 times the level of association detected at RARB exon 2 (data not shown). Each experiment was repeated at least three times, and the quantitative PCR analyses were performed in triplicate. The data are presented as percentages of input DNA (mean ± SE).

Pax3 binding sites (22) and displaying a putative complete site for RARα binding; (ii) the promoter region, located just upstream from the TSS and (iii) the genomic region located between RET enhancer and promoter (intervening sequences, IS). Activation of RET gene upon RA treatment was verified by quantitative reverse transcriptase PCR (qRT–PCR) in SK-N-BE cells (Supplementary Figure S1). Results of ChIP experiments showed that RARα was present, either in treated and untreated cells, on both promoter and enhancer regions and not on IS (Figure 1B). The amount of RARα protein bound to the enhancer region slightly increased after 12 h of RA treatment. These data suggest that RARα, although stably associated to RET regulatory regions, may promote transcription only in the presence of RA possibly by inducing changes of chromatin configuration. Then we performed luciferase transcriptional assays in order to investigate whether a 3.4-kb RET gene regulatory region, located upstream from TSS and including both promoter and enhancer, was sufficient for RA responsiveness. The results, shown in Figure 2A, demonstrated that plasmid constructs containing the 3.4-kb RET region upstream the luciferase gene were more active than empty plasmids (pGL3-basic); however, no significant increase of luciferase activity was observed when transfected cells were treated with RA. Then, DNA fragments of the RET enhancer region, containing either wild-type or mutated putative RARE, were cloned into the PGL3-promoter reporter plasmid that contains a SV40 promoter upstream from luciferase reporter gene. The transcriptional assays showed that the fragments containing the wild-type putative RARE behaved as an enhancer and promoted higher basal transcriptional activity, while this ability was lost when the RARE was disrupted (Figure 2B). However, neither the wild-type nor the mutated fragments were able to confer RA responsiveness to the reporter plasmids. Taken together, these results suggested that the presence of other genomic regions, not included in our constructs, were likely necessary for RA responsiveness possibly through the formation of chromatin loops that may bring together distant genomic regions and may account for the presence of RARα protein detected by our ChIP experiments at RET enhancer. In addition, possible epigenetic modification occurring at the endogenous gene, and not on transiently transfected constructs, may play a critical role in RA responsiveness. Thus, in order to investigate the relative contribution of RET 3.4-kb upstream region to RA responsiveness, we decided to investigate chromatin and DNA methylation changes that may occur at 3.4-kb RET regulatory region during RA-mediated activation.

### RA induces multiple epigenetic modifications restricted to RET promoter and enhancer

In order to study possible chromatin changes occurring during RET gene activation, we determined by a series of ChIP assays coupled with qRT–PCR, the histone modification state at the RET regulatory regions after different times of RA treatment. The major histone modifications were analyzed. First, we analyzed di- and trimethylated lysine 4 on histone H3 (H3K4me2, H3K4me3) whose increase is commonly associated with gene activation. Surprisingly, H3K4me2 levels were high prior to RA treatment and sharply decreased in concomitance with RET activation on both enhancer and promoter regions (Figure 3). However, at promoter region, such decrease was balanced by an increase of the trimethylated form (H3K4me3) while, at enhancer, no significant changes of H3K4me3 was observed. The specificity of these events for the regulatory regions was confirmed by the analysis of the same histone modifications at the IS, where no changes were observed (Figure 3). These results suggest that

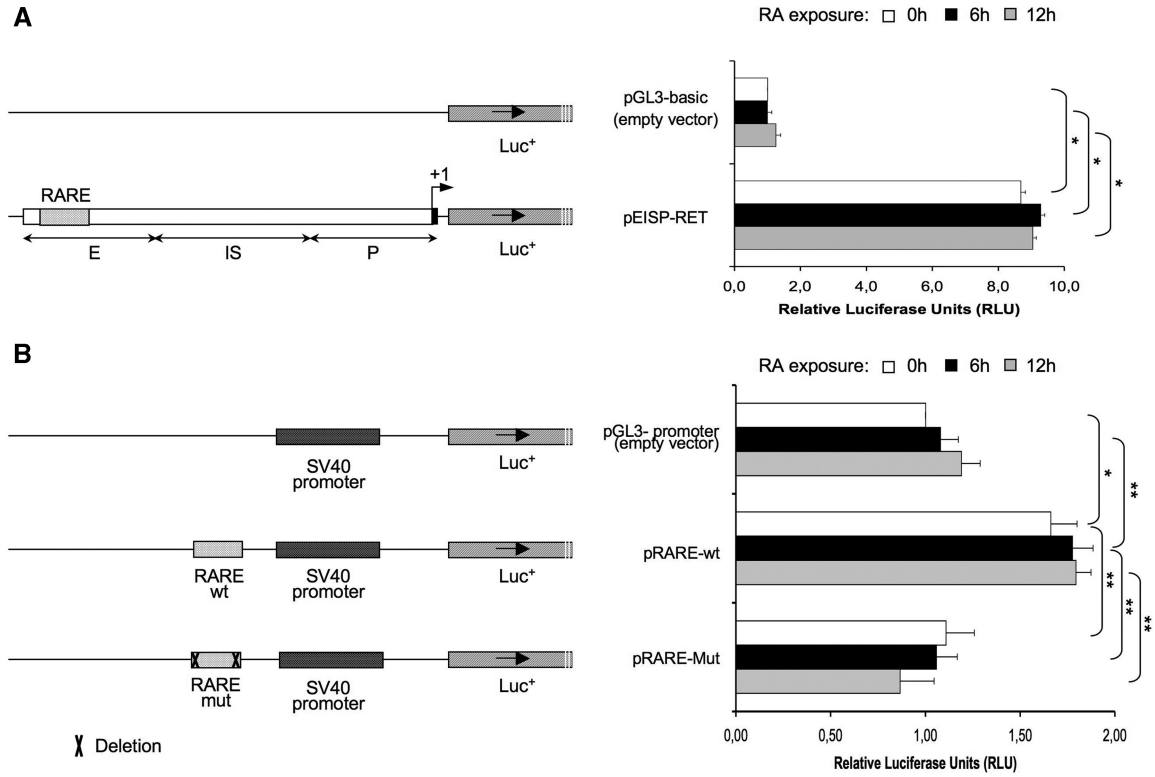


**Figure 2.** Transcriptional assays for RA responsiveness. (**A**) The region containing RET enhancer, intervening sequence and promoter (3.4 Kb) was amplified and cloned into pGL3-basic Luciferase Vector (pEISP-RET). Right panel: Relative Luciferase Assay results on SK-N-BE cells transfected with 200 μg of corresponding construct represented in the left panel. Plasmid constructs are described in 'Materials and Methods' section. (**B**) A 150-bp fragment including the putative RARE sequence identified on the basis of bioinformatic analysis was cloned both as wild-type (pRARE-wt) and in a mutated form (pRARE-Mut) in a pGL3-promoter Luciferase Vector. Two hundred micrograms of three different constructs were transfected into SK-N-BE cells (left panel): pGL3-promoter Luciferase Vector (empty); pGL3-promoter Luciferase Vector containing the putative RARE and pGL3-promoter Luciferase Vector containing the putative RARE lacking the triplette TCA in both DRs. Plasmid constructs are described in details in 'Materials and Methods' section. After transfection, cells were treated with RA (10 μM) for different times followed by luciferase activity determination. All tranfections were performed in triplicate; luciferase activity was detected 0, 6 and 12 h after RA exposure. Data are means ± SD of three independent experiments. E, Enhancer; IS, Intervening Sequences; P, Promoter; $*P < 0.01$; $**P < 0.05$.

consistent changes of methylation state of H3K4, that are specific for regulatory regions but differ between promoter and enhancer, accompany RET activation. In light of recent observations of cyclic histone modifications at estrogen- and androgen-regulated genes regulatory regions (28), it is interesting to note that the levels of H3K4me3 clearly cycled at RET promoter region during RA-mediated gene activation (Figure 3). Then, we analyzed the methylation state of H3K9 which is commonly considered a transcription repression marker (29). Results showed that the levels of both H3K9me2 and H3K9me3 strongly increased at the enhancer region during RA stimulation while no significant changes were observed at promoter region (Figure 3). Remarkably, the observed dynamics of H3K9 methylation at enhancer region, during the first 3 h of RA treatment, were in conflict with the widely reported role of these histone modifications as repressive markers. However, it is to be noted that after 6 h of RA treatment, H3K9me3 levels sharply decreased suggesting that the simultaneous increase of H3K9me2 levels was a consequence of H3K9me3 demethylation. Unlike H3K4me3, the changes in H3K9me2 and H3K9me3 levels did not appear to cycle during RA-mediated gene activation in the analyzed RET gene regions. The analysis of the IS region showed that no changes of H3K9me2 or H3K9me3 levels occurred upon RA treatment, thus confirming that the observed events were specific for the regulatory regions. Furthermore, we analyzed the levels of trimethylated H3K27 (H3K27me3) that are commonly associated with gene repression (30,31) and have been recently shown to play a role in RA response (32,33). Results of ChIP experiments showed that H3K27me3 was present at high levels only at the RET enhancer region in the absence of RA stimulation and a strong decrease of H3K27me3 accompanied RET gene activation. No significant changes of H3K27me3 were detected at IS nor at promoter regions. Finally, we analyzed the acetylation state of histone H3. As expected, although with a different dynamics, a cyclic increase of acetylation at both promoter and enhancer regions was observed during RA stimulation (Figure 3). Again, no changes of acetyl-H3 levels were detected at the IS confirming the specificity of the events observed at the enhancer and promoter regions. Interestingly, the levels of H3K27me3 and of acetyl-H3 clearly cycled at enhancer and promoter regions, respectively (Figure 3).

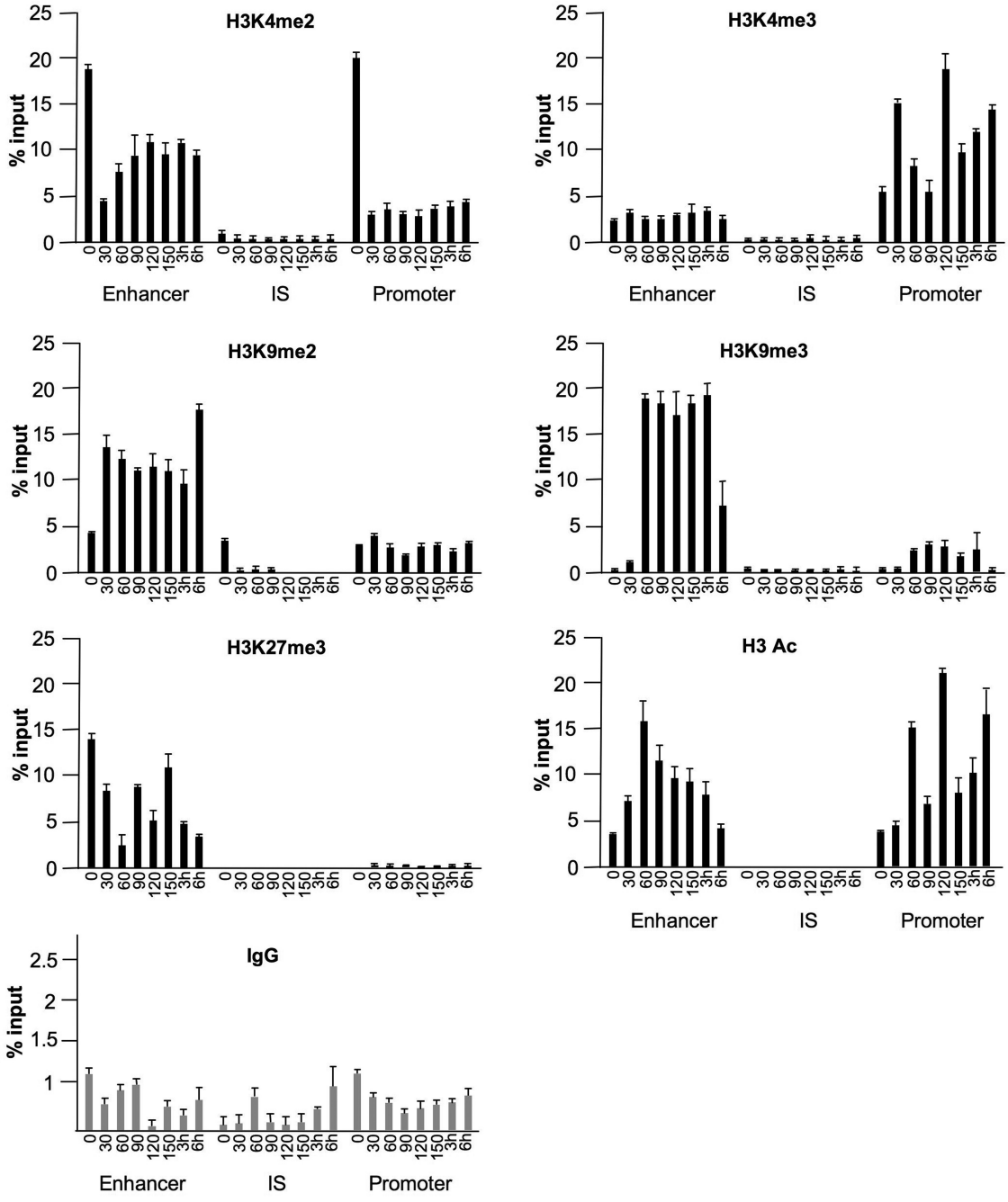


**Figure 3.** Dynamics of RA-dependent chromatin modifications at RET gene regulatory regions. SK-N-BE cells were treated for the indicated times with 10 μM RA and then cells were fixed with formaldehyde and processed into soluble chromatin. Chromatin samples were immunoprecipitated with the indicated antibodies and bound DNA was quantitated by real time PCR. Each experiment was repeated, starting with cell culture, at least three times, and the quantitative PCR analyses were performed in triplicate. The data are presented as percentages of input DNA (mean ± SE).

### RA induces the displacement of EZH2 and DNMTs from heavily methylated RET enhancer

The finding that the H3K27me3 levels play a key role in driving chromatin changes at enhancer region during RET gene activation prompted us to investigate whether EZH2, a H3K27 histone methyltransferase, was involved in RET transcriptional control. ChIP experiments using anti-EZH2 specific antibodies showed that, in untreated cells, EZH2 was present at high level on the enhancer region. These findings were consistent with the observed H3K27 methylation state at enhancer region. Upon RA treatment, the levels of EZH2 at enhancer region decreased together with the observed H3K27me3 demethylation (Figure 3). Interestingly, cycling of both H3K27me3 and EZH2 levels was observed after the initial decrease at the enhancer region. At promoter region, significant EZH2 binding was also detected (Figure 4).

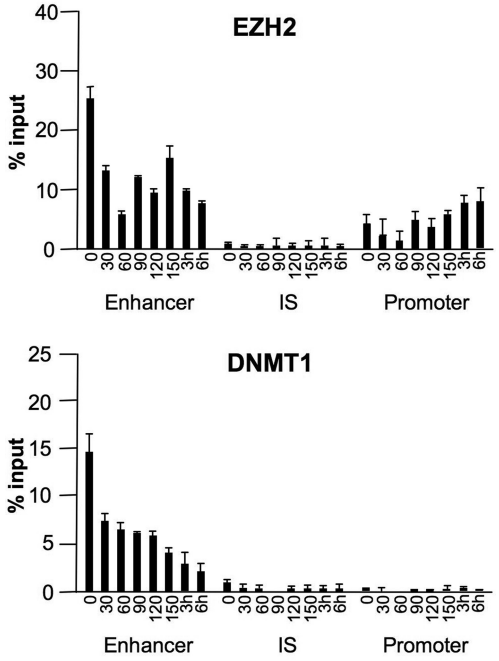


**Figure 4.** EZH2 and DNMT1 binding to RET regulatory regions. SK-N-BE cells were treated for the indicated times with 10 μM RA. ChIP experiments were performed using anti-EZH2 and anti-DNMT1 antibodies and bound DNA was quantitated by real time PCR. Data, presented as percentages of input DNA before immunoprecipitation, represent the results of three independent experiments ± SEMs.

Since EZH2 may act in concert with DNA methyltransferase (DNMTs), we performed additional ChIP analysis using DNMT1 and DNMT3b antibodies. During the same time-course, a binding behavior similar to that displayed by EZH2 was observed for DNMT1 (Figure 4) and DNMT3b (data not shown) at enhancer sequences while no consistent binding of both DNMTs was detected at both IS and promoter region upon RA treatment.

Taken together these results suggest that at promoter region EZH2 might be enzymatically inactive, possibly because the proteins to which EZH2 associates at promoter region differ from those associating at enhancer region. This hypothesis is also corroborated by the observation that DNMT1 and DNMT3b, that may be part of the Polycomb Repressor Complex (PRC2) to which EZH2 belongs (34), are recruited on the enhancer while are absent at the promoter region.

### DNA methylation state of RET gene

Next, because EZH2 association with DNMTs may have a role in the control of DNA methylation (34), we analyzed the DNA methylation state of RET regulatory genomic regions in SK-N-BE cells. A schematic representation of RET regulatory regions including CpG distribution and indication of the analyzed regions is shown in Figure 5A. Bisulfite genomic sequencing showed that enhancer region was heavily methylated while promoter region was almost unmethylated (Figure 5B) consistently with the observed differential localization of EZH2. In order to investigate whether the observed DNA methylation profiles at the RET locus were a specific feature of SK-N-BE cell line or resembled those present in human tissues, we analyzed both non-expressing (normal thyroid) and expressing (medullary thyroid carcinomas) human tissues. Results showed that CpG methylation at RET locus displayed a similar distribution among expressing, non-expressing tissues and SK-N-BE cells (Figure 5C). However, in medullary thyroid carcinomas the methylation degree at enhancer region was significantly lower compared to non-expressing thyroid tissue and SK-N-BE cells. Finally, treatment of SK-N-BE cells with a demethylating agent (5-aza-2-deoxyazacytidine), led to an increase of RET expression even in the absence of RA (Supplementary Figure S2). Overall, a possible interpretation of these data was that DNA methylation state of the RET enhancer region may contribute to gene repression in unstimulated cells and that full activation of RET gene may be achieved in RA-treated SK-N-BE cells by inducing chromatin remodelling at the heavily methylated enhancer region.

### RA induces displacement of MeCP2/HDAC1/Sin3A complex from RET enhancer facilitating transcription

We next investigated possible mechanisms allowing the observed modulation of chromatin configuration at enhancer region despite its heavily DNA methylated status. Since methyl-binding proteins are the major interpreters of DNA methylation exerting their role by binding to methylated DNA and promoting closed chromatin configuration, we hypothesized that these proteins could be involved in the regulation of RET gene. We performed ChIP experiments at different times of RA treatment of SK-N-BE cells using anti-MeCP2 and anti-MBD2 antibodies. While MBD2 was not present in the RET regulatory regions (data not shown), MeCP2 was specifically associated to the heavily methylated enhancer region (Figure 6A). Remarkably, upon RA treatment a strong decrease of MeCP2 binding to the enhancer region was observed in concomitance with RET activation. Since MeCP2 is frequently associated to a chromatin repressor complex including HDAC1 and Sin3A, we investigated the role of these proteins during RET activation by ChIP assays. We found that both HDAC1 and Sin3A were present on enhancer region before RA treatment and both were displaced in concomitance with RET activation (Figure 6B and C). These data are consistent with the hypothesis that RA may induce displacement of MeCP2 and associated proteins from methylated DNA favoring changes of chromatin configuration from closed to open state.

### Site-specific DNA demethylation at RET enhancer region follows RA treatment and interferes with MeCP2 binding

Next, we investigated whether the observed decrease of MeCP2 from the heavily methylated enhancer region upon RET activation could be associated to changes in DNA methylation state. We performed genomic bisulfite sequencing analysis to monitor the methylation degree of

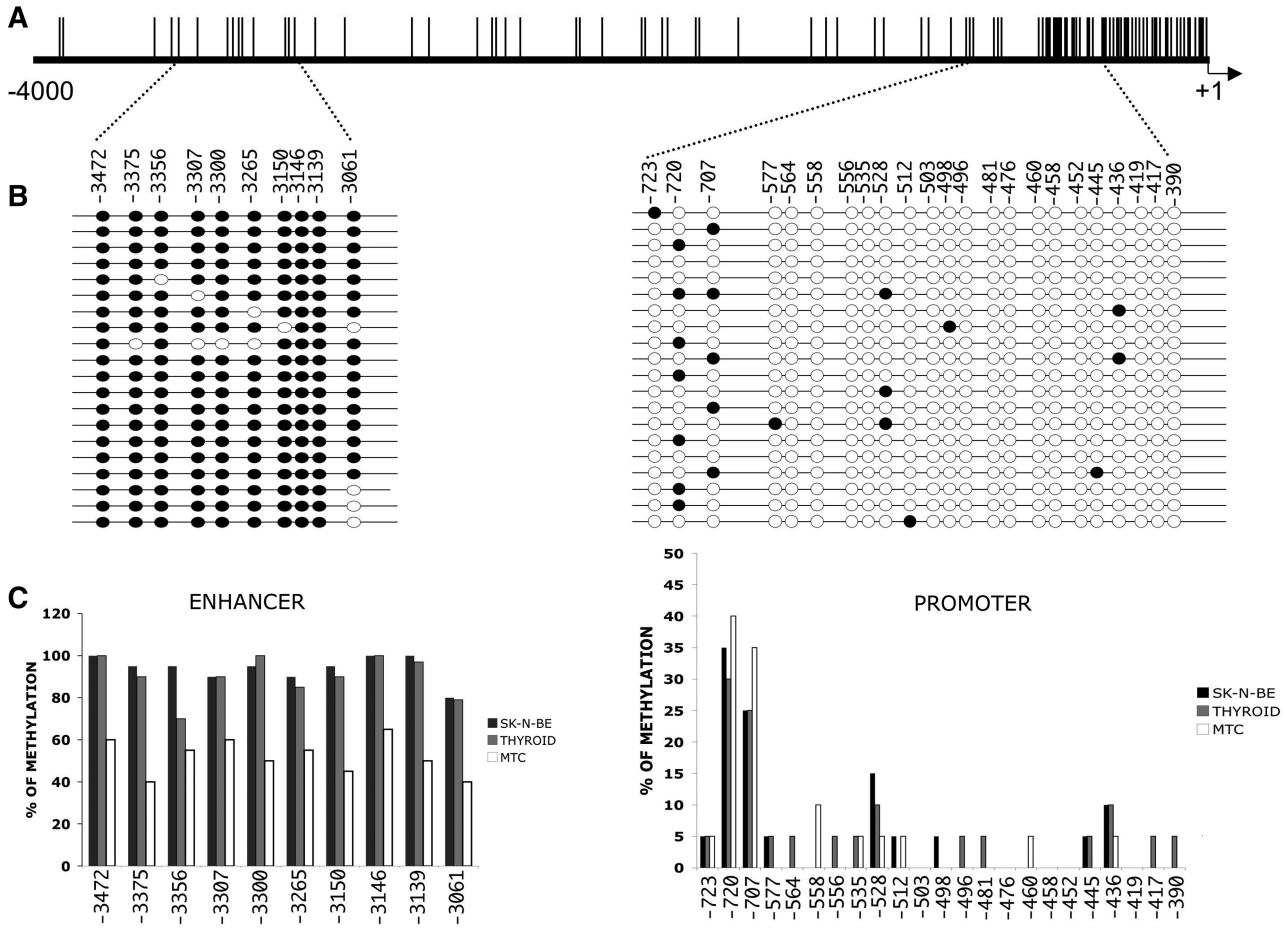


**Figure 5.** Methylation analysis of RET enhancer and promoter regions in SK-N-BE cells, human normal thyroid tissue and medullary carcinomas. (**A**) Schematic representation of CpG distribution at RET regulatory regions. Each vertical bar indicates the relative position of a CpG site. Transcription start site is indicated (+1). The specific regions analyzed for DNA methylation state are indicated by horizontal bars. Primers used for enhancer (EbiF and EbiR) and promoter (PbiF and PbiR) methylation analysis are reported in 'Materials and Methods' section. (**B**) DNA methylation patterns in individual PCR clones from the RET enhancer and promoter. All the sequenced molecules from SK-N-BE cells are shown. Numbers on top show the location of CpG dinucleotides. Black circles indicate that the corresponding cytosines are methylated. (**C**) Percentage of DNA methylation at individual CpG sites in the RET gene enhancer (left panel) and promoter (right panel) in SK-N-BE cells, human normal thyroid tissue (thyroid) and medullary thyroid carcinoma (MTC). Data, from the sequence analysis of least 20 plasmid clones for each sample, were compiled by individual CpG dinucleotides and expressed as the ratio of methyl-C to the number of clones. Positions of CpG sites relative to transcription initiation site are given below the bars.

10 CpG sites within the enhancer region (from −3502 to −3023) at different times after RA treatment. Very interestingly, we found that starting at 1 h, a specific CpG sites (position −3375) underwent partial demethylation (Figure 7 and data not shown). These data were confirmed by independent quantitative methylation analyses using MassARRAY and pyrosequencing techniques (Figure 7 and data not shown). Next, in order to investigate *in vivo* whether the methylation state of −3375 CpG site had some influence on MeCP2 binding to the enhancer region, we performed a ChIP using anti-MeCP2 antibody followed by bisulfite methylation analysis (ChIP-BA) (24). Results shown in Figure 7C indicated that, after 3 h of RA treatment of SK-N-BE cells, DNA molecules immunoprecipitated with MeCP2 displayed 100% of methylation at −3375 CpG site while in the input DNA the methylation degree at the same site was 50%. Interestingly, the methylation state of the two adjacent CpG sites remained almost constant. These results suggest that the unmethylated state of −3375 site in the RET enhancer region can interfere with MeCP2 binding.

Next, in order to confirm an active role of MeCP2 in RET gene silencing in cells not treated with RA, we performed MeCP2 knock-down experiments. SK-N-BE cells were transfected with MeCP2 specific siRNA and the mRNA expression of RET and MeCP2 (as a control) were measured by qRT-PCR (Figure 8A). We found that MeCP2 mRNA levels were reduced to about 30% of initial levels while RET expression showed a 3-fold increase even in the absence of RA treatment (Figure 8A). Finally, we evaluated by ChIP analysis, the occupancy of MeCP2 at the enhancer region after the SK-N-BE cells were treated with 5-Azacytidine, a DNA demethylating agent. SK-N-BE cells were treated with 10 μM or 50 μM 5-aza-2-deoxyazacytidine for 48 h. As a

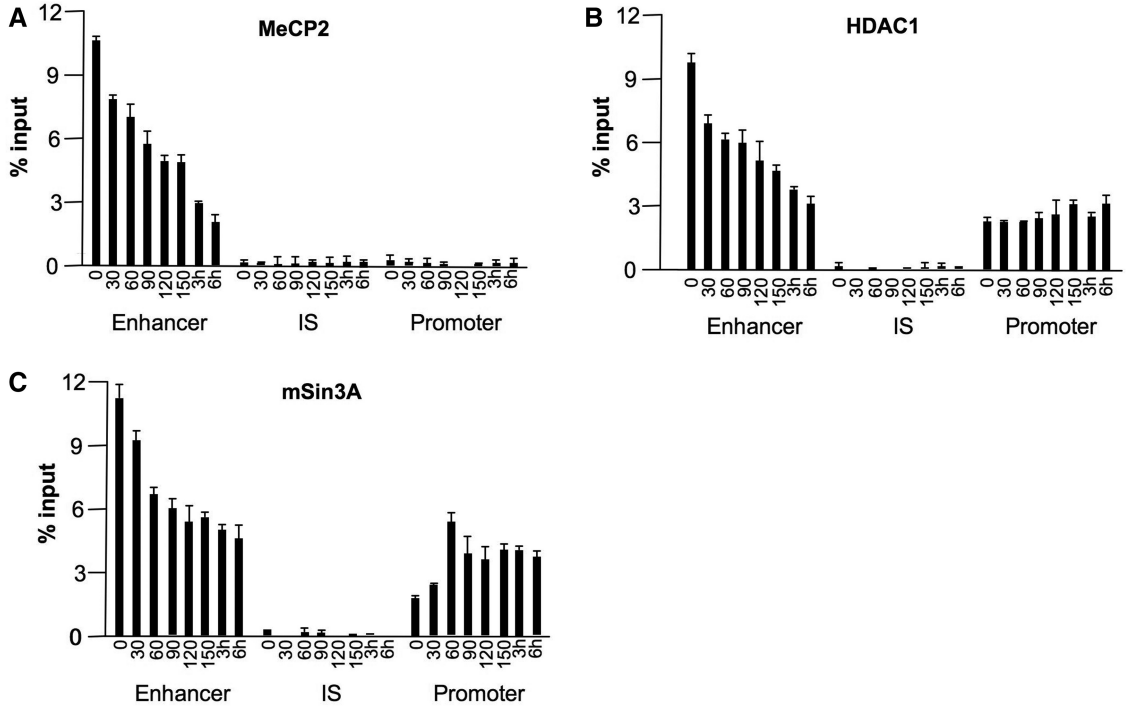


**Figure 6.** Association of MeCP2 repression complex with RET gene regulatory regions. SK-N-BE cells were treated for the indicated times with 10 μM RA. ChIP experiments were performed using anti-MeCP2 (**A**), anti HDAC1 (**B**) and anti mSin3A (**C**) antibodies. Bound DNAs were quantitated by real time PCR. Data, presented as percentages of input DNA before immunoprecipitation, represent the results of three independent experiments ± standard error of the means.

control, we found by bisulphite analysis that the average DNA methylation of 10 CpG sites located in the enhancer region decreased from 93 to 25% and 16%, respectively. In these conditions, as demonstrated by ChIP experiments shown in Figure 8B, the levels of MeCP2 bound to the enhancer region were found to be drastically reduced. Overall, these data support the hypothesis that RA induces changes in DNA methylation state of specific CpG sites at RA responsive genes which, in turn, favor the release of MeCP2 and, consequently of the chromatin repressor complex.

## DISCUSSION

In this work we have performed for the first time a systematic analysis of the main epigenetic modifications accompanying RET gene activation in a neuroblastoma cell line upon RA stimulation. First, we found that a 3.4-kb region upstream from TSS and containing a putative RARE, although not sufficient to provide RA responsiveness in luciferase reporter assays, instead, in the genomic context could bind RARα and was subject to several chromatin and DNA methylation changes upon RA-mediated RET activation. We found that, for some aspects, the chromatin dynamics did not follow the general rules described for genes activated by different nuclear receptors, such as estrogen or androgen receptors which, in contrast to RA responsive genes, have been thoroughly investigated (14,15). Most of reports indicate that increase in H3K4me2 and acetyl-H3 as well as decrease in H3K9me3 and H3K27me3 levels mark transcriptionally active chromatin structure. Our results indicate that the primary epigenetic determinants of RA-induced RET activation differ between enhancer and promoter regions. At promoter region, the main driver of RET activation appears to be the increase of H3K4me3 levels while no significant changes of the methylation state of H3K27 and H3K9 were observed. Acetylation of histone H3 increased at both enhancer and promoter regions in concomitance with RET activation, which is in agreement with previous reports (20). At RET enhancer region we observed a simultaneous presence of histone modifications associated with transcriptional repression (H3K27me3) and activation (H3K4me2) (Figure 3). Interestingly, genomic regions containing this so called 'bivalent chromatin domain' have been recently mapped and shown to be associated in particular with developmental genes and with highly conserved noncoding elements (35). We show that during RA treatment the prominent epigenetic modification at RET enhancer region was the demethylation of H3K27me3, while H3K9me3 demethylation occurred at later times (6 h of RA exposure) following an initial consistent increase observed in the earlier phases (Figure 3). A significant demethylation of H3K4me2 was also observed at the enhancer region. A similar chromatin dynamics, including demethylation of H3K27me3, has been recently described for other RA regulated loci (Hoxa1, Cyp26A1 and RARb2) in F9 embryonal carcinoma cells (13). However, in this study it was observed that H3K4me2 levels remained constant during RA treatment while the methylation state of H3K9 was not investigated. A possible explanation of the non-conventional

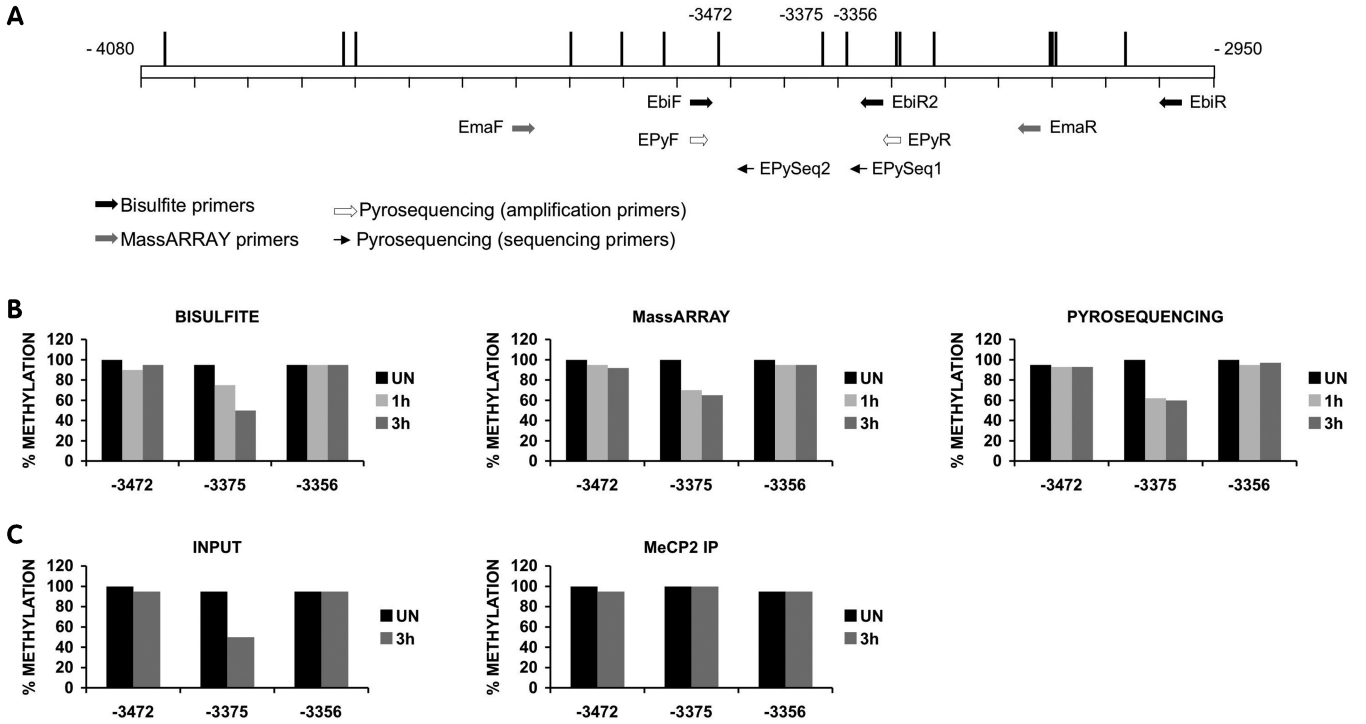


**Figure 7.** Demethylation of a specific CpG site at RET gene enhancer region upon RA treatment. (**A**) Schematic representation of CpG distribution at RET enhancer. Each vertical bar indicates the relative position of a CpG site. The approximate position of the primers utilized for bisufite, MassARRAY and pyrosequencing quantitative methylation analyses are indicated (see 'Materials and Methods' section for primer specifications). Numbering is referred to TSS. (**B**) SK-N-BE cells were left untreated (UN) or treated with RA for the indicated times and then methylation analyses were performed on bisulfite treated genomic DNA. Data shown represent the results of three independent methods for quantitative methylation analyses (bisulfite, manual genomic sequencing; Sequenom MassARRAY quantitative methylation analysis; Pyrosequencing quantitative methylation analysis). For manual genomic sequencing, data, from the sequence analysis of at least 20 plasmid clones for each sample, were compiled by individual CpG dinucleotides and expressed as the ratio of methyl-C to the number of clones. Further details for Sequenom MassARRAY and pyrosequencing are reported in 'Materials and Methods' section. The results for three CpG sites including the −3375 and adjacent CpG sites, according the three different procedures, are shown as percentage of DNA methylation at individual CpG sites in the RET gene enhancer. (C) ChIP followed by bisulfite analysis (ChIP-BA). SK-N-BE cells were treated with RA for 3 h (3 h) or left untreated (UN) and then ChIPs were performed using anti-MeCP2 antibodies. Input and immunoprecipitated DNAs were subjected to genomic sequencing bisulfite methylation analysis using EBiF and EbiR2 primers (see 'Materials and Methods' section). Data were from the sequence analysis of at least 20 plasmid clones for each sample and expressed as the ratio of methyl-C to the number of clones. Shown are the percentages of methylation of three CpG sites.

modifications observed at RET gene enhancer is that the DNA methylation state of this region might influence the chromatin dynamics during the transition from a repressive to an active state. In fact, our data show that RET enhancer region is heavily methylated in SK-N-BE cells and it is well established that dense CpG methylation has a direct impact on local chromatin state, a connection which is mediated by methyl-binding proteins that retain the ability to recruit chromatin repressor complexes on methylated DNA. Thus, it is likely that chromatin changes occurring at highly methylated genomic regulatory regions in the course of gene activation may follow different rules from those occurring at low methylated or unmethylated regions. In this work we have then addressed different questions regarding the role of DNA methylation in the control of RET gene expression. First we found that heavily methylated state of RET enhancer was not a specific feature of the cell line used in this study since a similar distribution of CpG methylation status it was observed in human tissues. However, we observed that medullary carcinomas, which constitutively express RET gene, showed an average methylation degree at 12 CpG sites in the enhancer region of 60% versus an average of 90% observed in non-expressing thyroid tissues and in SK-N-BE cells in which RET expression is inducible by RA (Figure 5). All these data together with the observed ability of demethylating drugs to partially reactivate RET gene in SK-N-BE even in the absence of RA stimulation, led us to conclude that DNA methylation at enhancer region may contribute to RET gene repression even though this repressive state may be overcome by RA-induced epigenetic modifications. Secondly, the simultaneous presence at RET enhancer of H3K27me3 modification and highly methylated CpGs status prompted us to investigate a possible role of EZH2, a component of PRC2/3 complex, in the determination of such epigenetic features at RET locus. In fact, EZH2 is a H3K27 methyltransferase that has been shown to drive DNMTs at its target loci (34). Moreover, we observed that the levels of EZH2 bound to enhancer region significantly decreased upon RA treatment of SK-N-BE cells in concomitance with decreased H3K27me3 levels and gene activation. These data strongly suggest that alleviation of PcG repression may play a critical role in RA-mediated

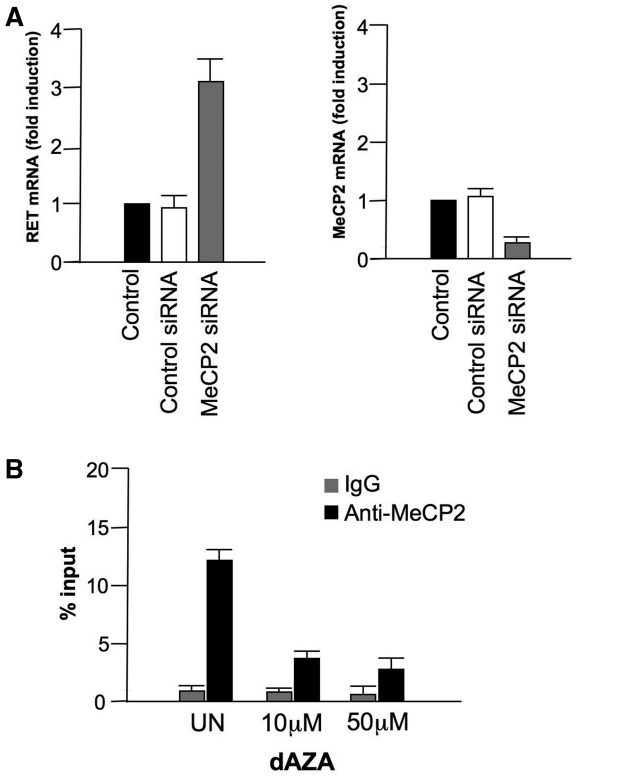


**Figure 8.** MeCP2 contribution to RET gene silencing. (**A**) MeCP2 knock-down. SK-N-BE cells were transfected with MeCP2 or a negative control siRNA and after 48 h the RET and MeCP2 mRNA levels were analyzed by RT–PCR. Results are expressed as fold induction compared with control untransfected cells (Control). The experiments were repeated three times and quantitative PCR analyses were performed in triplicates. Error bars represent standard deviation. (**B**) Effects of 5-aza-2-deoxyazacytidine on MeCP2 binding to RET enhancer. SK-N-BE cells were treated with 5-aza-2-deoxyazacytidine (dAZA) for 48 h at the indicated concentrations and were immunoprecipitated with anti-MeCP2 antibodies (black bar). Anti-IgG were used as a negative control (gray bar). The MeCP2 binding to RET enhancer was quantitated by real-time PCR. Data, presented as percentages of input DNA, represent the results of three independent experiments ± standard error of the means.

RET activation. Another interesting aspect emerging from our data is that the levels of some histone modifications cycled at RET gene during RA-mediated activation. The levels of the main active marks, H3K4me3 and H3ac, clearly cycle at promoter region. Interestingly, these two active marks behave anti-correlated at early time-points (30–60 min) while they correlate at later time points. In addition, the levels of EZH2 were shown to cycle at enhancer region and correlate with the H3K27me3 levels.

Finally, because it is largely believed that densely methylated DNA region correspond to highly compacted chromatin configuration, we worked on the hypothesis that changes of DNA methylation state or modulation of the association of methyl-binding proteins to methylated DNA were necessary for chromatin transition from a closed to an open state. In previous works, we found that MBD2 binding to methylated DNA, and not DNA methylation state, may be affected by the presence of other proteins leading to reactivation of methylated genes (36,37). In this work we found that MBD2 is not involved in RET gene regulation but we demonstrate that both a site-specific CpG demethylation and the release of MeCP2 from methylated RET enhancer accompanied changes of histone modifications and RET gene activation. An active role of −3375 CpG site demethylation in favoring MeCP2 release is supported by the analysis of methylation state of this CpG site in MeCP2 immunoprecipitated DNA showing an enrichment in DNA bearing methylated −3375 CpG site compared to input DNA (Figure 7) and by the observation that this CpG site showed a low methylation degree in the RET expressing tissues (Figure 5). Very interestingly, a similar mechanism has been well established for the activation of brain derived nerve-growth factor (BDNF) gene in rat neurons following calcium influx (38–40). In this case, the release of MeCP2 from BDNF promoter (promoter IV) is necessary for transcriptional activation and appears to be mediated by both a site-specific CpG demethylation (38,40) and by phosphorylation, by a CaMKII-dependent mechanism, of a specific residue (S421) of MeCP2 protein (39). The possibility that post-translational modification of MeCP2 could be involved also in the RA-induced release of MeCP2 from methylated RET enhancer and, possibly, other RA target loci, deserves to be explored. In any case, the observed displacement of MeCP2 from RET enhancer may not only facilitate the transcriptional activation but also help to establish and stabilize a reprogramming of gene expression following RA exposure. At this stage, our data support a novel intriguing mechanisms in which RA induces changes in DNA methylation state of specific CpG sites at RA responsive genes that, in turn, favor the release of MeCP2 and, consequently of the chromatin repressor complex. In this scenario, the heavily methylated state of RET enhancer region, found in both expressing and non-expressing tissues, would represent an epigenetic regulatory feature of RET enhancer rather than a simple repressive signal. The possible active involvement of MeCP2 binding in the regulation of methylated RA target genes, as suggested by our data, could have important implications both in normal development and in neurodevelopmental disorders and deserves further investigations.

## SUPPLEMENTARY DATA

Supplementary Data are available at NAR Online.

## FUNDING

Research grants from MIUR, Italian Ministry of University and Research, and AIRC, Associazione Italiana per la Ricerca sul Cancro. Funding for open access charge: Department of Cellular and Molecular Biology and Pathology.

*Conflict of interest statement*. None declared.

## REFERENCES


1. Duester,G. (2008) Retinoic acid synthesis and signaling during early organogenesis. *Cell*, **134**, 921–931.
2. Mark,M., Ghyselinck,N.B. and Chambon,P. (2006) Function of retinoid nuclear receptors: lessons from genetic and pharmacological dissections of the retinoic acid signaling pathway during mouse embryogenesis. *Annu. Rev. Pharmacol. Toxicol.*, **46**, 451–480.
3. Means,A.L. and Gudas,L.J. (1995) The roles of retinoids in vertebrate development. *Annu. Rev. Biochem.*, **64**, 201–233.
4. Mongan,N.P. and Gudas,L.J. (2007) Diverse actions of retinoid receptors in cancer prevention and treatment. *Differentiation*, **75**, 853–870.
5. Germain,P., Chambon,P., Eichele,G., Evans,R.M., Lazar,M.A., Leid,M., De Lera,A.R., Lotan,R., Mangelsdorf,D.J. and Gronemeyer,H. (2006) International Union of Pharmacology. LX. Retinoic Acid Receptors. *Pharmacol. Rev.*, **58**, 712–725.
6. McKenna,N.J. and O'Malley,B.W. (2002) Combinatorial control of gene expression by nuclear receptors and coregulators. *Cell*, **108**, 465–474.
7. Hartman,H.B., Yu,J., Alenghat,T., Ishizuka,T. and Lazar,M.A. (2005) The histone-binding code of nuclear receptor co-repressors matches the substrate specificity of histone deacetylase 3. *EMBO Rep.*, **6**, 445–451.
8. Glass,C.K. and Rosenfeld,M.G. (2000) The coregulator exchange in transcriptional functions of nuclear receptors. *Genes Dev.*, **14**, 121–141.
9. Rochette-Egly,C. (2005) Dynamic combinatorial networks in nuclear receptor-mediated transcription. *J. Biol. Chem.*, **280**, 32565–32568.
10. Lefebvre,B., Ozato,K. and Lefebvre,P. (2002) Phosphorylation of histone H3 is functionally linked to retinoic acid receptor beta promoter activation. *EMBO Rep.*, **3**, 335–340.
11. Ju,B.G., Lunyak,V.V., Perissi,V., Garcia-Bassets,I., Rose,D.W., Glass,C.K. and Rosenfeld,M.G. (2006) A topoisomerase IIbeta-mediated dsDNA break required for regulated transcription. *Science*, **312**, 1798–1802.
12. Mainguy,G., In der Rieden,P.M., Berezikov,E., Woltering,J.M., Plasterk,R.H. and Durston,A.J. (2003) A position-dependent organisation of retinoid response elements is conserved in the vertebrate Hox clusters. *Trends Genet.*, **19**, 476–479.
13. Gillespie,R.F. and Gudas,L.J. (2007) Retinoid regulated association of transcriptional co-regulators and the polycomb group protein SUZ12 with the retinoic acid response elements of Hoxa1, RARbeta(2), and Cyp26A1 in F9 embryonal carcinoma cells. *J. Mol. Biol.*, **372**, 298–316.
14. Métivier,R., Penot,G., Hübner,M.R., Reid,G., Brand,H., Kos,M. and Gannon,F. (2003) Estrogen receptor-alpha directs ordered, cyclical, and combinatorial recruitment of cofactors on a natural target promoter. *Cell*, **115**, 751–763.
15. Perillo,B., Ombra,M.N., Bertoni,A., Cuozzo,C., Sacchetti,S., Sasso,A., Chiariotti,L., Malorni,A., Abbondanza,C. and Avvedimento,E.V. (2008) DNA oxidation as triggered by H3K9me2 demethylation drives estrogen-induced gene expression. *Science*, **319**, 202–206.
16. Sidell,N. (1982) Retinoic acid-induced growth inhibition and morphologic differentiation of human neuroblastoma cells *in vitro*. *J. Natl Cancer Inst.*, **68**, 589–596.
17. Sidell,N., Altman,A., Haussler,M.R. and Seeger,R.C. (1983) Effects of retinoic acid (RA) on the growth and phenotypic expression of several human neuroblastoma cell lines. *Exp. Cell Res.*, **148**, 21–30.
18. Reynolds,C.P., Matthay,K.K., Villablanca,J.G. and Maurer,B.J. (2003) Retinoid therapy of high-risk neuroblastoma. *Cancer Lett.*, **197**, 185–192.
19. Oppenheimer,O., Cheung,N.K. and Gerald,W.L. (2007) The RET oncogene is a critical component of transcriptional programs associated with retinoic acid-induced differentiation in neuroblastoma. *Mol. Cancer Ther.*, **6**, 1300–1309.
20. Puppo,F., Griseri,P., Fanelli,M., Schena,F., Romeo,G., Pelicci,P., Ceccherini,I., Ravazzolo,R. and Patrone,G. (2002) Cell-line specific chromatin acetylation at the Sox10-Pax3 enhancer site modulates the RET proto-oncogene expression. *FEBS Lett.*, **523**, 123–127.
21. Puppo,F., Musso,M., Pirulli,D., Griseri,P., Bachetti,T., Crovella,S., Patrone,G., Ceccherini,I. and Ravazzolo,R. (2005) Comparative genomic sequence analysis coupled to chromatin immunoprecipitation: a screening procedure applied to search for regulatory elements at the RET locus. *Physiol. Genomics*, **23**, 269–274.
22. Lang,D. and Epstein,J.A. (2003) Sox10 and Pax3 physically interact to mediate activation of a conserved c-RET enhancer. *Hum. Mol. Genet.*, **12**, 937–945.
23. Livak,K.J. and Schmittgen,T.D. (2001) Analysis of relative gene expression data using real-time quantitative PCR and the 2(-Delta Delta C(T)) Method. *Methods*, **25**, 402–408.
24. Matarazzo,M.R., Lembo,F., Angrisano,T., Ballestar,E., Ferraro,M., Pero,R., De Bonis,M.L., Bruni,C.B., Esteller,M., D'Esposito,M. *et al.* (2004) In vivo analysis of DNA methylation patterns recognized by specific proteins: coupling CHIP and bisulfite analysis. *Biotechniques*, **37**, 666–668, 670, 672, 673.
25. Ehrich,M., Nelson,M.R., Stanssens,P., Zabeau,M., Liloglou,T., Xinarianos,G., Cantor,C.R., Field,J.K. and van den Boom,D. (2005) Quantitative high-throughput analysis of DNA methylation patterns by base-specific cleavage and mass spectrometry. *Proc. Natl Acad. Sci. USA*, **102**, 15785–15790.
26. Chambon,P. (1996) A decade of molecular biology of retinoic acid receptors. *FASEB J.*, **10**, 940–954.
27. Kato,S., Sasaki,H., Suzawa,M., Masushige,S., Tora,L., Chambon,P. and Gronemeyer,H. (1995) Widely spaced, directly repeated PuGGTCA elements act as promiscuous enhancers for different classes of nuclear receptors. *Mol. Cell. Biol.*, **15**, 5858–5867.
28. Métivier,R., Penot,G., Hübner,M.R., Reid,G., Brand,H., Kos,M. and Gannon,F. (2003) Estrogen receptor-alpha directs ordered, cyclical, and combinatorial recruitment of cofactors on a natural target promoter. *Cell*, **115**, 751–763.
29. Stancheva,I. (2005) Caught in conspiracy: cooperation between DNA methylation and histone H3K9 methylation in the establishment and maintenance of heterochromatin. *Biochem. Cell Biol.*, **83**, 385–395.
30. Margueron,R., Trojer,P. and Reinberg,D. (2005) The key to development: interpreting the histone code? *Curr. Opin. Genet. Dev.*, **15**, 163–176.
31. Schubert,D., Primavesi,L., Bishopp,A., Roberts,G., Doonan,J., Jenuwein,T. and Goodrich,J. (2006) Silencing by plant Polycomb-group genes requires dispersed trimethylation of histone H3 at lysine 27. *EMBO J.*, **25**, 4638–4649.
32. Lee,M.G., Villa,R., Trojer,P., Norman,J., Yan,K.P., Reinberg,D., Di Croce,L. and Shiekhattar,R. (2007) Demethylation of H3K27 regulates polycomb recruitment and H2A ubiquitination. *Science*, **318**, 447–450.
33. Villa,R., Pasini,D., Gutierrez,A., Morey,L., Occhionorelli,M., Viré,E., Nomdedeu,J.F., Jenuwein,T., Pelicci,P.G., Minucci,S. *et al.* (2007) Role of the polycomb repressive complex 2 in acute promyelocytic leukemia. *Cancer Cell*, **11**, 513–525.
34. Viré,E., Brenner,C., Deplus,R., Blanchon,L., Fraga,M., Didelot,C., Morey,L., Van Eynde,A., Bernard,D., Vanderwinden,J.M. *et al.* (2006) The Polycomb group protein EZH2 directly controls DNA methylation. *Nature*, **439**, 871–874.
35. Bernstein,B.E., Mikkelsen,T.S., Xie,X., Kamal,M., Huebert,D.J., Cuff,J., Fry,B., Meissner,A., Wernig,M., Plath,K. *et al.* (2006) A bivalent chromatin structure marks key developmental genes in embryonic stem cells. *Cell*, **125**, 315–326.
36. Lembo,F., Pero,R., Angrisano,T., Vitiello,C., Iuliano,R., Bruni,C.B. and Chiariotti,L. (2003) MBDin, a novel MBD2-interacting protein, relieves MBD2 repression potential and reactivates transcription from methylated promoters. *Mol. Cell Biol.*, **23**, 1656–1665.
37. Angrisano,T., Lembo,F., Pero,R., Natale,F., Fusco,A., Avvedimento,V.E., Bruni,C.B. and Chiariotti,L. (2006) TACC3

mediates the association of MBD2 with histone acetyltransferases and relieves transcriptional repression of methylated promoters. *Nucleic Acids Res*., **34**, 364–372.
38. Martinowich,K., Hattori,D., Wu,H., Fouse,S., He,F., Hu,Y., Fan,G. and Sun,Y.E. (2003) DNA methylation-related chromatin remodeling in activity-dependent BDNF gene regulation. *Science*, **302**, 890–893.
39. Chen,W.G., Chang,Q., Lin,Y., Meissner,A., West,A.E., Griffith,E.C., Jaenisch,R. and Greenberg,M.E. (2003) Derepression of BDNF transcription involves calcium-dependent phosphorylation of MeCP2. *Science*, **302**, 885–889.
40. Wade,P.A. (2004) Dynamic regulation of DNA methylation coupled transcriptional repression: BDNF regulation by MeCP2. *Bioessays*, **26**, 217–220.